Centre for Nanoscale BioPhotonics
ARC CENTRE OF EXCELLENCE

Creating windows into the body

Multilayer resonator sensitivity analysis

Jonathan M. M. Hall

ARC Georgina Sweet Laureate Team:
S. Afshar V., M. R. Henderson, A. François, T. Reynolds, N. Riesen and T. M. Monro

ANZCOP 30 Nov – 3 Dec 2015

Australian Government
Australian Research Council
THE UNIVERSITY of ADELAIDE
MACQUARIE University SYDNEY · AUSTRALIA
RMIT UNIVERSITY

Introduction

- **Resonators** have emerged as a platform for novel sensor design.
- They involve trapping light inside microscopic devices such as spheres, disks or bubbles.
- **What for?** Resonators can act as detectors of nearby macromolecules such as viruses, bacteria and DNA, and changes in the refractive index inside or outside the resonator.

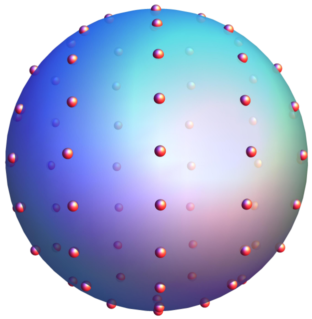

- **How?** Resonators of a diameter of ten to several hundred microns can support **whispering gallery modes** (WGMs), which are sensitive to the environment.

Australian Government
Australian Research Council
THE UNIVERSITY of ADELAIDE
MACQUARIE University SYDNEY · AUSTRALIA
RMIT UNIVERSITY

Whispering gallery modes

Underlying principles

- Whispering gallery modes are bound electromagnetic waves that travel around the surface of a resonator.
- The waves resonate only at certain 'modes' as they are reflected around the surface.
- The modes correspond to the number of surface nodes, and radial nodes.
- The width (wavelength range) of the modes can be very narrow (high Q-factor), and easily tracked.
- At the material interface, an 'evanescent field' extends into the medium, and is sensitive to changes.

Whispering gallery modes

Example spectrum

- The WGMs appear as sharp peaks in the power spectrum. TE & TM modes shown for a single dipole excitation.

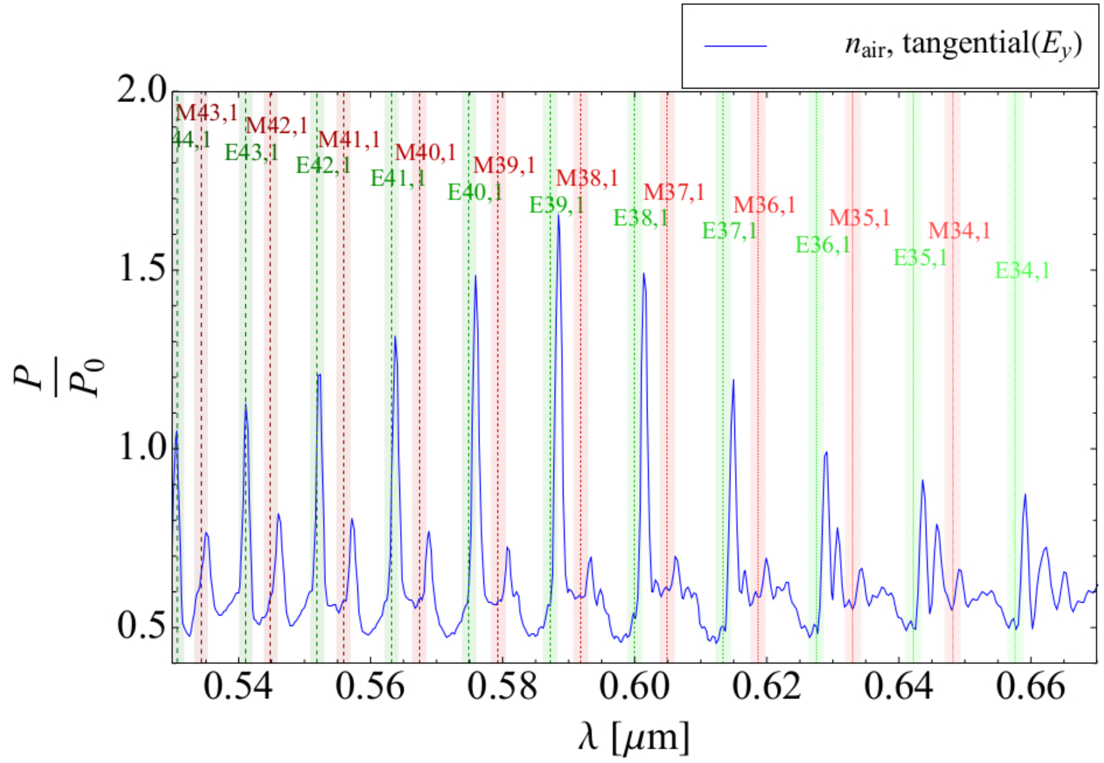

Australian Government
Australian Research Council
THE UNIVERSITY of ADELAIDE
MACQUARIE University SYDNEY·AUSTRALIA
RMIT UNIVERSITY

Resonator simulators

Approaches in the literature

- Simulating modes inside resonators is useful for **preselecting optimal configurations** for biosensing.
- Microbubbles, 1-layer and multilayer resonators demonstrate **improved sensitivity**, and small mode volume.
- Early models focus on simulating the **mode positions only**. Then spectra for dipoles embedded in spherical droplets[1] allowed direct comparison with experiment. Although Mie scattering theory has been extended to the multilayer case[2], recent thin-layer studies[3] are still **unable to generate spectra**.

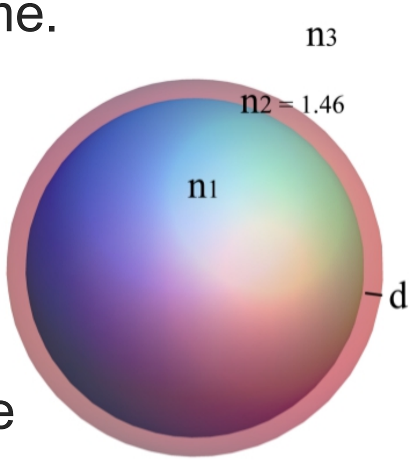

[1] H. Chew, M. Kerker, and P. J. McNulty, J. Opt. Soc. Am. 66, 440–444 (1976).
[2] W. Liang, Y. Xu, Y. Huang, A. Yariv, J. Fleming, S.-Y. Lin, Opt. Express 12, 657–669 (2004).
[3] I. Teraoka and S. Arnold, J. Opt. Soc. Am. B 23, 1434–1441 (2006).

Australian Government
Australian Research Council
THE UNIVERSITY of ADELAIDE
MACQUARIE University SYDNEY·AUSTRALIA
RMIT UNIVERSITY

The transfer matrix approach

Advantages

- We build on the **transfer matrix approach**[4], which harmonises previous models in the literature, and incorporates the ability to generate spectra.
- Our model is able to simulate the **mode positions** and the **spectra** for a given dipole source or multiple sources placed anywhere in the medium, for a **multilayer sphere** of any number of layers.
- We can also simulate the spectra for a uniform distribution of dipoles (acting as an **active medium**) in any layer.
- The spectra are **fast** to produce (~100 ms/λ) and stability issues have been addressed.

[4] A. Moroz, Annals of Physics 315, 352 – 418 (2005).

Australian Government
Australian Research Council
THE UNIVERSITY of ADELAIDE
MACQUARIE University SYDNEY·AUSTRALIA
RMIT UNIVERSITY

Excitation scenarios

Theory

- The TE and TM mode positions determined by coefficients A, B, C, D.

$$\mathbf{E}_i = \sum_{l,m} \left(\frac{\imath c}{n_i^2\omega}\right) A_i \nabla \times [\mathbf{Y}_{llm}(\theta,\phi) j_l(k_i r)] + \left(\frac{\imath c}{n_i^2\omega}\right) B_i \nabla \times [\mathbf{Y}_{llm}(\theta,\phi) n_l(k_i r)] + C_i \mathbf{Y}_{llm}(\theta,\phi) j_l(k_i r) + D_i \mathbf{Y}_{llm}(\theta,\phi) n_l(k_i r)$$

$$\mathbf{B}_i = \sum_{l,m} A_i \mathbf{Y}_{llm}(\theta,\phi) j_l(k_i r) + B_i \mathbf{Y}_{llm}(\theta,\phi) n_l(k_i r) - \left(\frac{\imath c}{\omega}\right) C_i \nabla \times [\mathbf{Y}_{llm}(\theta,\phi) j_l(k_i r)] - \left(\frac{\imath c}{\omega}\right) D_i \nabla \times [\mathbf{Y}_{llm}(\theta,\phi) n_l(k_i r)]$$

For TM **transfer matrix:**
(TE: $n^2 \to \mu$, $\mu \to 1$)

$$M_i(r) = \begin{pmatrix} \frac{1}{\mu_i} j(k_i r) & \frac{1}{\mu_i} h^{(1)}(k_i r) \\ \frac{1}{n_i^2}[k_i r\, j(k_i r)]' & \frac{1}{n_i^2}[k_i r\, h^{(1)}(k_i r)]' \end{pmatrix}$$

$M_{i+1}(r).x_{i+1} = M_i(r).x_i$, where $x=(A,B)^T$ (TE) or $(C,D)^T$ (TM).

- For the simple case of a sphere, the coeff cients can be calculated by doing a single matrix inversion: $x_{i+1} = M^{-1}_{i+1}(r).M_i(r).x_i = \mathbf{T}.x_i$

Geometric mode positions

- For N layers, **T** (N+1->0) becomes generalised to:

$$M_{N+1}^{-1}(r_N)M_N(r_N)M_N^{-1}(r_{N-1})M_{N-1}(r_{N-1})M_{N-1}^{-1}(r_{N-2})M_{N-2}(r_{N-2})\ldots M_2^{-1}(r_1)M_1(r_1)M_1^{-1}(r_0)M_0(r_0)$$

- If we call **S** the inverse of **T**, we find the relations:

$B_{N+1} = A_0\, S_{21}/\det(S)$ (TE) $\quad D_{N+1} = -C_0\, S_{21}/\det(S)$ (TM)

$A_{N+1} = -A_0\, S_{22}/\det(S)$ (TE) $\quad C_{N+1} = C_0\, S_{22}/\det(S)$ (TM)

- If there are no sources, the mode positions can be determined geometrically by the ratios of B_{N+1}/A_{N+1} and D_{N+1}/C_{N+1}, which diverge near a resonance.

Australian Government Australian Research Council
THE UNIVERSITY of ADELAIDE
MACQUARIE University SYDNEY · AUSTRALIA
RMIT UNIVERSITY

Excitation scenarios

Single dipole source

- For a dipole source in a layer *i*, the coefficients x_i get a contribution a_{iH}, and x_{i+1} get a contribution a_{iL}, for TE and TM.

$$a_{iEL}(r_i') = 4\pi(k_i^2/n_i)\sqrt{\frac{\mu_i}{\epsilon_i}}\,\mathbf{P}.\nabla\times[h_l^{(1)}(k_i r_i')\mathbf{X}^*_{\mathrm{lm}}(\theta_i',\phi_i')] = 4\pi(k_i^2/\epsilon_i)\mathbf{P}.\nabla\times[h_l^{(1)}(k_i r_i')\mathbf{X}^*_{lm}(\theta_i',\phi_i')]; \quad a_{iML}(r_i') = 4\pi\imath k_i^3\frac{1}{\epsilon_i}h_l^{(1)}(k_i r_i')\mathbf{P}.\mathbf{X}^*_{lm}(\theta_i',\phi_i')$$

$$a_{iEH}(r_i') = 4\pi(k_i^2/n_i)\sqrt{\frac{\mu_i}{\epsilon_i}}\,\mathbf{P}.\nabla\times[j_l(k_i r_i')\mathbf{X}^*_{\mathrm{lm}}(\theta_i',\phi_i')] = 4\pi(k_i^2/\epsilon_i)\mathbf{P}.\nabla\times[j_l(k_i r_i')\mathbf{X}^*_{\mathrm{lm}}(\theta_i',\phi_i')]; \quad a_{iMH}(r_i') = 4\pi\imath k_i^3\frac{1}{\epsilon_i}j_l(k_i r_i')\mathbf{P}.\mathbf{X}^*_{lm}(\theta_i',\phi_i')$$

- By adding these into the coeff cients, we can get the total power spectrum:

$$r^2\int \mathbf{S}_{SC}.\hat{\mathbf{r}}d\Omega = \frac{c}{8\pi}\sqrt{\frac{\epsilon_{N+1}}{\mu_{N+1}}}\frac{1}{k_{N+1}^2}\sum_{l,m}[(\frac{1}{n_{N+1}^2})|B_{N+1}|^2 + |D_{N+1}|^2]$$

$$P_{total} = \frac{c}{2}\sqrt{\frac{\epsilon_{N+1}}{\mu_{N+1}}}\frac{k_j^4 n_j^2}{n_{N+1}^2}\frac{1}{\epsilon_j^2}\sum_l 2l+1\left\{(\frac{n_j^2}{n_{N+1}^2})l(l+1)\frac{\left|[\alpha_l j_l(k_j r_j') - \beta_l h_l^{(1)}(k_i r_i')]\right|^2}{k_j^2 r_j'^2}|\mathbf{P}_r|^2 + \left[(\frac{n_j^2}{n_{N+1}^2})\frac{\left|\{\alpha_l \frac{\mathrm{d}}{\mathrm{d}r}[r_j' j_l(k_j r_j')] - \beta_l\frac{\mathrm{d}}{\mathrm{d}r}[r_j' h_l(k_j r_j')]\}\right|^2}{k_j^2 r_j'^2} + \left|[\gamma_l j_l(k_i r_i') - \zeta_l h_l^{(1)}(k_i r_i')]\right|^2\right](\frac{|\mathbf{P}_\theta|^2+|\mathbf{P}_\phi|^2}{2})\right\}$$

$\alpha_l = (t_{22} - \frac{S_{21}}{S_{22}}t_{12})$ and $\beta_l = (t_{21} - \frac{S_{21}}{S_{22}}t_{11})$

$\gamma_l = (t_{44} - \frac{S_{43}}{S_{44}}t_{34})$ and $\zeta_l = (t_{43} - \frac{S_{43}}{S_{44}}t_{33})$

- For a dipole in layer *j*, and for *t* = **T** (j->0).

Australian Government
Australian Research Council

THE UNIVERSITY of ADELAIDE

MACQUARIE University SYDNEY·AUSTRALIA

RMIT UNIVERSITY

Excitation scenarios

Single dipole source

- By plotting the normalised power, P/P_0, across a range of wavelengths, in the simple case of a sphere (no additional layers) we find our result matches the Chew model exactly!
- Diam=6 μm, n=1.59 (polystyrene).
- Ex indicates the radial portion, Ey the tangential portion.

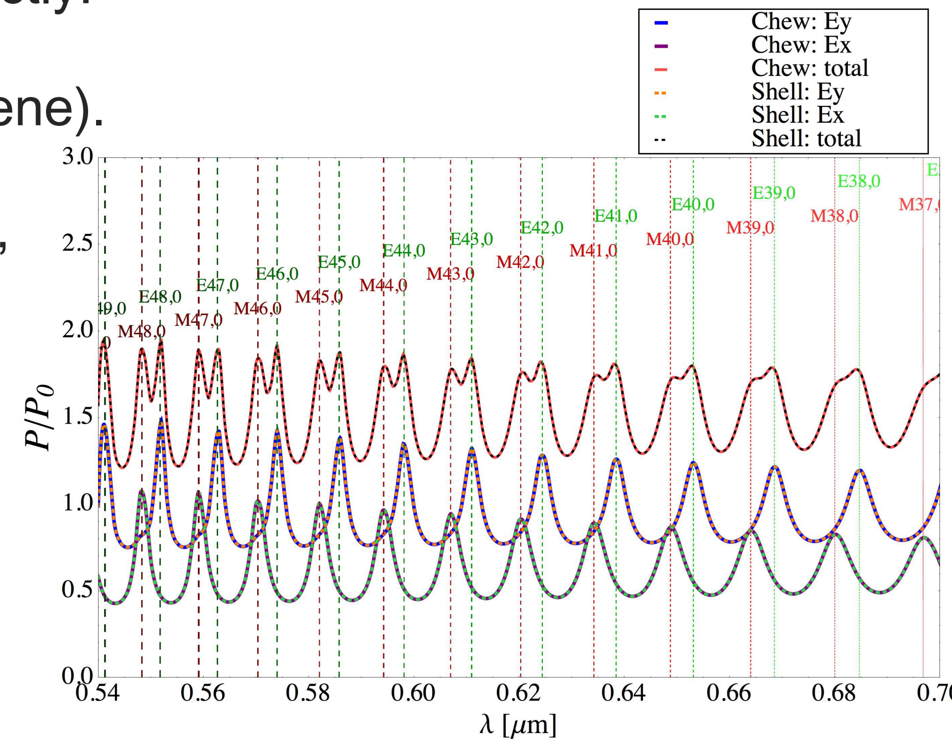

Australian Government
Australian Research Council
THE UNIVERSITY of ADELAIDE
MACQUARIE University SYDNEY·AUSTRALIA
RMIT UNIVERSITY

Excitation scenarios

Uniform distribution of dipoles

- For an active layer, the averaged power spectum is:

$$\frac{1}{3}\left\langle \frac{P_{\perp}}{P_{\perp}^{0}} \right\rangle + \frac{2}{3}\left\langle \frac{P_{\parallel}}{P_{\parallel}^{0}} \right\rangle = \frac{1}{2}\sqrt{\frac{\epsilon_{N+1}}{\mu_{N+1}}}\frac{n_j^2}{n_{N+1}^2}\frac{n_j}{k_j^2\epsilon_j V_{jshell}}4\pi\sum_l\left[(\frac{n_j^2}{n_{N+1}^2})l(l+1)I_l^{(1)} + (\frac{n_j^2}{n_{N+1}^2})I_l^{(2)} + I_l^{(3)} \right]$$

where:

$$\frac{1}{(2l+1)}\left[l(l+1)I_l^{(1)} + I_l^{(2)}\right] = l(l+1)\int_{jregion}\left|[\alpha_l j_l(k_j r_j') - \beta_l h_l^{(1)}(k_i r_i')]\right|^2 dr_j' + \int_{jregion}\left|\{\alpha_l \frac{\mathrm{d}}{\mathrm{d}r}[r_j' j_l(k_j r_j')] - \beta_l \frac{\mathrm{d}}{\mathrm{d}r}[r_j' h_l(k_j r_j')]\}\right|^2 dr_j'$$

$$I_l^{(3)} = (2l+1)\int_{jregion} k_j^2 r_j'^2 \left|[\gamma_l j_l(k_i r_i') - \zeta_l h_l^{(1)}(k_i r_i')]\right|^2 dr_j'$$

- V_{jshell} is the total volume of the layer.
- The total power can also be plotted versus wavelength.

Excitation scenarios

Uniform distribution of dipoles

- For the simple case of a sphere, our result also matches the Chew model.

- Furthermore, we have mathematically shown that our result for a single thin layer over a microsphere is exactly the same as the Arnold model.

- This is encouraging for the plausibility of our model in the general case of multiple layers.

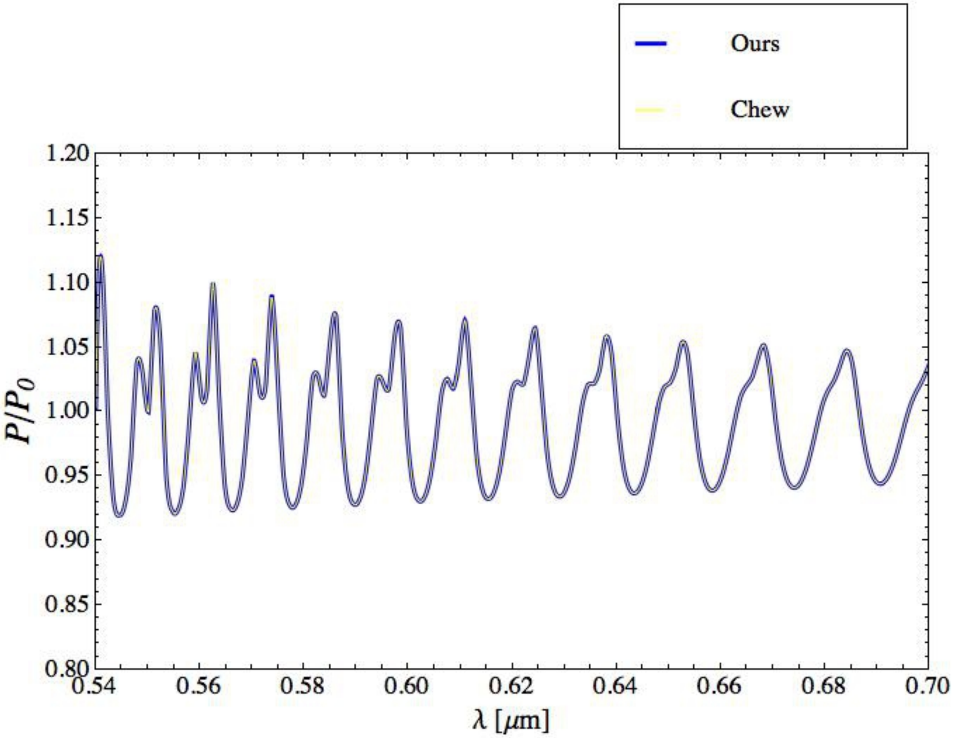

Results

Single-layer shell

- We apply the model to the case of a spherical silica microsphere (n=1.452, D=15 μm) coated with a thin layer of a high refractive index material (n=1.7). The surrounding medium is water.

- As the thickness of the layer, *d* is changed from 10-50 nm, the Purcell factor increases as the layer thickness is increased.

- The mode positions shift minutely over this range of *d*.

- Note that the peak heights are not uniformly increased as *d* is changed.

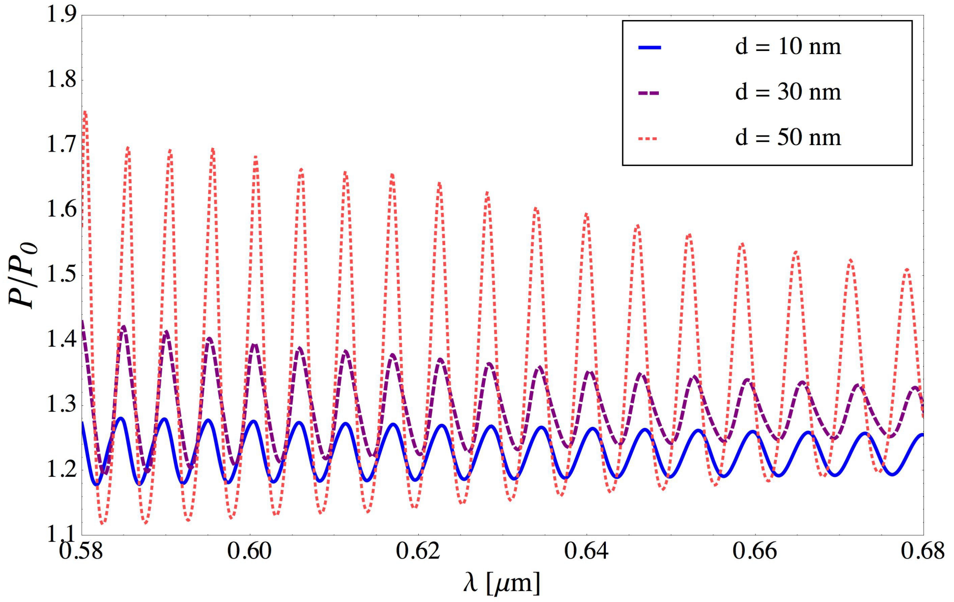

Sensitivity analysis

- We can conduct a sensitivity analysis by changing the index of the surrounding medium and tracking the changes in the WGM peaks.

- The layer thickness is kept constant at 50 nm. As the surrounding index is increased from 1.33 to 1.37, a systematic shift in the peak positions to the right is found, inaddition to a suppressed Purcell factor.

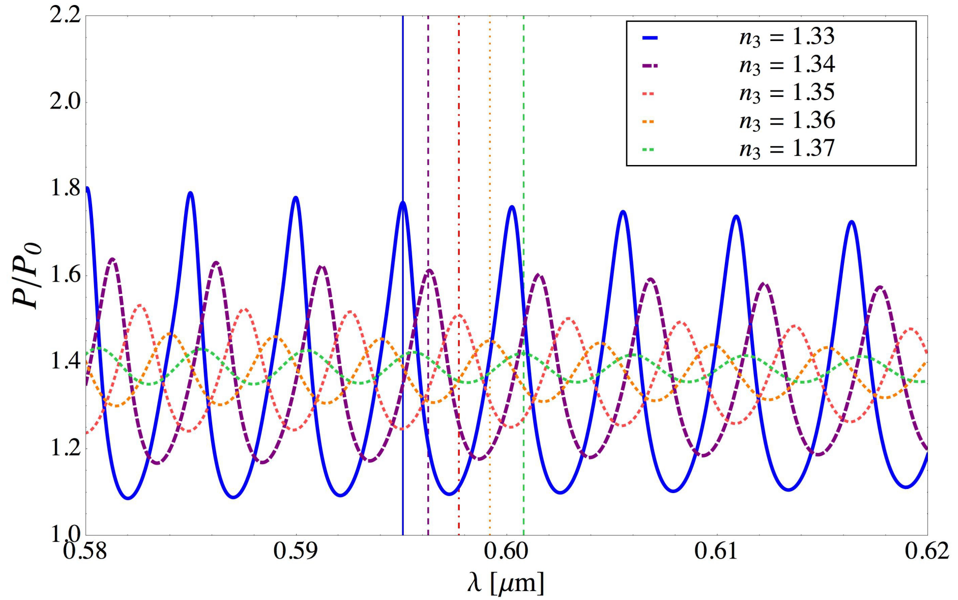

- By averaging the wavelength shift for several increments, a sensitivity of Δλ/Δn = 1.433 nm/R.I.U. is estimated.

Australian Government
Australian Research Council
THE UNIVERSITY of ADELAIDE
MACQUARIE University SYDNEY·AUSTRALIA
RMIT UNIVERSITY

Conclusion

A fast and robust multilayer spectrum generator

- We have developed a new model that is able to generate whispering gallery mode spectra for a multilayer resonator, using the transfer matrix approach.

- The model is able to accommodate one or more dipole sources, or a uniform distribution of sources in any layer.

- The model has been tested against known results in the literature for the limiting cases of sphere and single-layer resonators and it matches.

- A preliminary analysis on a microsphere with a high refractive index layer shows changes in the Purcell factor and mode positions, which allow a clear assessment of the sensitivity of the resonator.

Australian Government
Australian Research Council
THE UNIVERSITY of ADELAIDE
MACQUARIE University SYDNEY·AUSTRALIA
RMIT UNIVERSITY